

Generation and detection of ultrabroadband terahertz radiation using photoconductive emitters and receivers

Y. C. Shen, P. C. Upadhyaya, H. E. Beere, and E. H. Linfield^{a)}

Cavendish Laboratory, University of Cambridge, Madingley Road, Cambridge CB3 0HE, United Kingdom

A. G. Davies

School of Electronic and Electrical Engineering, University of Leeds, Leeds LS2 9JT, United Kingdom

I. S. Gregory, C. Baker, W. R. Tribe, and M. J. Evans

TeraView Ltd., Unit 302/304 Cambridge Science Park, Milton Road, Cambridge, CB4 0WG United Kingdom

(Received 3 February 2004; accepted 10 May 2004)

We report the coherent generation and detection of ultrabroadband terahertz (THz) radiation using low-temperature-grown GaAs photoconductive antennas as both emitters and receivers. THz radiation with frequency components over 15 THz was obtained, the highest reported for a THz time-domain system based on photoconductive antennas. Such a system has a smooth spectral distribution between 0.3 and 7.5 THz, ideal for spectroscopic applications. In addition, sharp spectral features at 8.0 and 8.8 THz were observed, and explained in terms of optical phonon resonances in the photoconductive antennas. © 2004 American Institute of Physics.

[DOI: 10.1063/1.1768313]

The coherent generation and detection of terahertz (THz) radiation using ultrashort optical pulses has been investigated intensively during the last decade. The pulse width of commercially available mode-locked Ti:sapphire lasers is approaching 10 fs and, with such ultrashort laser pulses, the spectral distribution of the detected THz radiation has been reported to be over 30 THz, using thin electro-optic (EO) crystals as the emitter and detector.^{1,2} In contrast, the spectral bandwidth of THz time-domain spectroscopy systems³ employing photoconductive (PC) antennas, the main alternative for generating and detecting coherent THz radiation, has been limited to ~ 3 THz.^{4,5} This limited bandwidth of PC antennas was originally explained by either the finite carrier lifetime or the momentum relaxation time of the carriers in the substrate. However, low-temperature-grown GaAs (LT-GaAs) PC antennas have recently been used to detect ultrabroadband (over 30 THz) electromagnetic radiation generated by optical rectification of ultrashort laser pulses in thin EO crystals.^{6,7} The fast response of the PC receivers was explained by the fast rise time of the photogenerated carrier concentration, which is determined by the laser pulse width.⁶ Very recently we also observed ultrabroadband (over 30 THz) THz emission from LT-GaAs PC antennas, using a 20- μm -thick ZnTe crystal as the THz sensor.⁸ Pronounced THz emission, originating from optical phonon oscillations in GaAs ($\nu_{\text{TO}} \equiv 8.02$ THz; $\nu_{\text{LO}} \equiv 8.76$ THz) was also observed, and the shape of the measured THz signal was further complicated by the phonon resonances of the ZnTe detector ($\nu_{\text{TO}} \equiv 5.3$ THz; $\nu_{\text{LO}} \equiv 6.2$ THz).

In this letter, we report the first system combining a PC antenna emitter and a PC antenna receiver for the generation and electric-field-resolved detection of ultrabroadband THz radiation. The measured THz signal has a smooth spectral distribution from 0.3 to 7.5 THz, ideal for spectroscopic applications. Furthermore, the coherent optical phonon oscillations

in the GaAs antennas are directly observed with a high time resolution, with the frequency and decay time of the coherent oscillations being determined by fitting the experimental results with an exponentially decaying sine wave.

The general experimental arrangement for coherent generation and detection of ultrabroadband THz radiation has been described previously.⁸ In brief, a Ti:sapphire laser provides visible/near-infrared pulses of 15 fs duration at a center wavelength of 790 nm with a repetition rate of 76 MHz. The output is split into two parts: a 400 mW beam is focused onto the surface of a biased LT-GaAs PC emitter for THz generation, and a 30 mW beam serves as the probe beam to gate the PC receiver antenna for THz detection. The PC emitter has a gap of 400 μm , and is biased using an 11 kHz chopped sinusoidal wave with peak amplitude ± 120 V. For both PC emitter and receiver, the NiCr/Au electrodes (Ti/Pd/Au for receiver) are vacuum-evaporated on a 1.0- μm -thick LT-GaAs layer grown at 220 °C on a 0.53-mm-thick semi-insulating GaAs substrate. *Ex situ* post-growth annealing of the LT-GaAs (see Ref. 9) allowed optimization of the carrier lifetimes and resistivities for the individual PC receiver and emitter. Specifically, the carrier lifetimes for the receiver and emitter are 0.1 and 10 ps, respectively, as determined from transient reflectance measurements.⁹ The laser pulse width incident on the PC emitter and receiver is estimated to be 20 fs.

The emitted THz pulse is collimated and focused onto the sample by a pair of parabolic mirrors. The transmitted THz pulse is then collected and focused using another pair of parabolic mirrors onto the surface of a LT-GaAs antenna for PC detection. It should be noted that the geometry used for PC generation and detection is critical. Following the technique in Ref. 8, the THz radiation generated in the PC emitter is collected in a reflection geometry [see Fig. 1(a)], thereby avoiding absorption and dispersion in the GaAs substrate. This is essential for observing the high frequency components of the generated THz radiation. Another advantage of such a configuration is that the back of the GaAs

^{a)}Electronic mail: eh110@cam.ac.uk

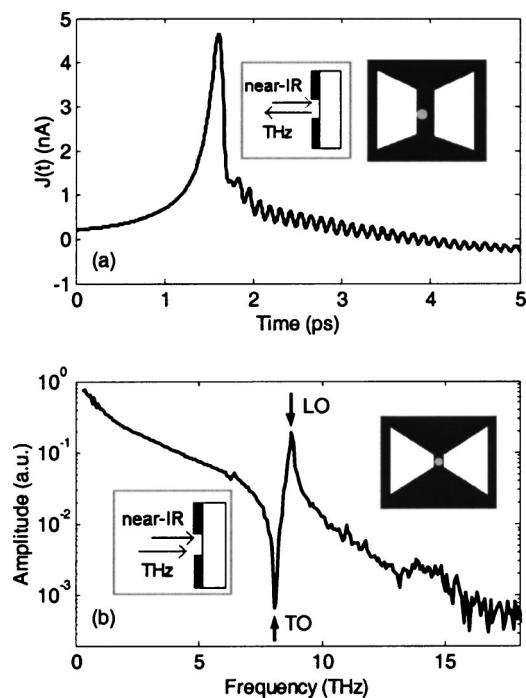


FIG. 1. (a) Temporal THz waveform and, (b) its corresponding Fourier transform amplitude spectrum. The arrows mark spectral features corresponding to TO and LO (phonons of the GaAs $\nu_{\text{TO}} \equiv 8.02$ THz; $\nu_{\text{LO}} \equiv 8.76$ THz) crystal. Inset of (a) shows the schematic geometry of the biased and asymmetrically excited LT-GaAs PC emitter (antenna gap of $400 \mu\text{m}$); (b) shows the schematic geometry of an LT-GaAs PC receiver (blunted bowtie antenna: $8 \mu\text{m}$ gap, 90° bow angle, $8 \mu\text{m}$ length).

substrate is free to be modified to minimize THz reflections (and thus increase the spectral resolution of the obtained THz spectra), or for cooling schemes⁵ to be added. THz detection was achieved using the geometry shown in Fig. 1(b), with once again absorption and dispersion in the GaAs substrate minimized. In all measurements, the variable delay stage, which provides the time delay between the THz pulse and the probe pulse, is scanned over a distance of 2 mm, providing a spectral resolution of 75 GHz (2.5 cm^{-1}). The whole apparatus is enclosed in a vacuum-tight box, which is purged with dry nitrogen gas to reduce the effects of water vapor absorption. Measurements are performed at room temperature.

Figure 1(a) shows a typical temporal THz waveform generated from the PC emitter and detected with the PC receiver, with Fig. 1(b) showing the corresponding frequency spectrum. In the frequency domain, the spectrum of the THz radiation extends continuously to over 15 THz, except for a spectral dip at 8 THz and a distinct peak at 8.7 THz. These two spectral features are explained as originating from longitudinal-optical (LO) and transverse-optical (TO) phonon resonances in the GaAs PC antennas. In the time domain, the phonon oscillations can be seen immediately after the initial transient, and extend over 12 ps. These oscillations were fitted with an exponentially-decaying sine wave: $E_{\text{THz}}(t) = C_1 e^{-t/\tau} \sin(2\pi\nu t - C_2)$. As shown in Fig. 2, the agreement between the fitted and the measured THz signal is very good. The best-fit results give an oscillating frequency $\nu = 8.7$ THz and a decay time $\tau = 3$ ps, confirming that these oscillations originate from LO phonon resonances in the GaAs ($\nu_{\text{LO}} \equiv 8.76$ THz).

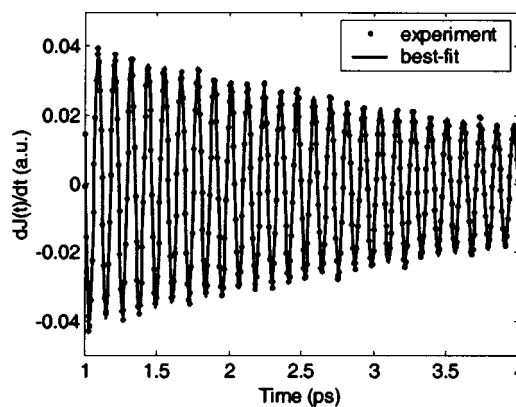


FIG. 2. Measured (points) and calculated (curve) temporal THz waveform between 1.0–4.0 ps. Note that the phonon oscillations can be seen immediately after the initial transient [see Fig. 1(a)], and extend over 12.0 ps, although for clarity, only a restricted interval is shown here.

Ultrabroadband PC detection was first demonstrated by Kono *et al.*⁶ using, for THz generation, optical rectification of a femtosecond laser pulse in a $100\text{-}\mu\text{m}$ -thick ZnTe crystal (i.e., EO generation and PC detection). The amplitude of the THz electric field measured in our work is about two orders of magnitude larger (four orders of magnitude larger in THz power) than that reported by Kono *et al.*,⁶ owing to the larger power available from the PC emitter. Therefore, the combination of a PC emitter and a PC receiver antenna proves an ideal THz system for practical spectroscopy applications. As an example, Fig. 3 shows the vibrational spectrum of maltose measured with such a system. Samples were prepared by mixing finely milled maltose polycrystalline powder (Sigma Aldrich Co.) with polyethylene powder (Sigma Aldrich Co.) in a mass ratio of 1:10, and then compressing the mixture to form a pellet of thickness 1.3 mm. The low frequency vibrational modes of maltose were previously measured with a conventional THz time-domain spectrometer, but the frequency range was limited to 0.3–3.0 THz.¹⁰ In contrast, here we resolved 14 vibrational modes over a much wider frequency range (0.3–7.3 THz), demonstrating the extended bandwidth of this THz spectroscopy system. Note, that these

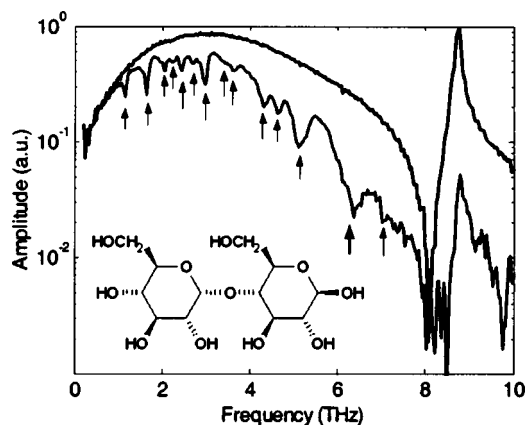


FIG. 3. Fourier-transform amplitude spectrum of the THz radiation measured after transmitting through a pure polyethylene reference pellet (upper trace), and a maltose/polyethylene sample pellet (lower trace). Arrows indicate vibrational modes of maltose at frequencies of 1.11, 1.61, 2.0, 2.21, 2.39, 2.64, 2.93, 3.33, 3.6, 4.28, 4.61, 5.07, 6.35, and 7.0 THz. Note that the Fourier transforms were performed using the first derivatives of the measured signals, to minimize the possible spectral artefacts caused by an offset in the measured signals. Inset shows the molecular structure of maltose.

observed vibrational modes correspond to both inter- and intra-molecular interactions.¹¹

In a previous study,⁸ we used EO detection with a 20- μm -thick ZnTe crystal to study THz radiation from a similar LT-GaAs antenna (PC-generation and EO detection). The measured THz signals, however, were far more complicated, with two additional spectral features at 5.3 and 6.2 THz. It is clear that these two additional spectral features were caused by the ZnTe detector ($\nu_{\text{TO}} \equiv 5.3$ THz; $\nu_{\text{LO}} \equiv 6.2$ THz) used in previous studies. On the other hand, the THz signals measured in the previous study⁸ covered a broader (over 30 THz) spectral range. The reduced spectral coverage in the present study is mainly a result of the decreased sensitivity of the PC antennas at high frequencies. For the EO detection employed in Ref. 8, the EO crystal detects the polarization change of the probe beam induced by the THz electric field in the sensor crystal. Therefore, the detected signal is simply proportional to the THz electric field. For PC detection of ultrabroadband THz radiation, the PC antenna works as an integrating detector. The photocurrent from the antenna, $J(t)$, is proportional to the time integration of the product of the incident THz electric field, $E(t)$, and the total number of photo-generated carriers, $N(t)$, in the PC antenna: $J(t) = e\mu \int_{-\infty}^{\infty} E_{\text{THz}}(t')N(t'-t)dt'$ where e is the electron charge and μ is the electron mobility in the LT-GaAs. Therefore, for an ideal PC antenna with ultrashort carrier lifetime, $J(\omega) \propto E_{\text{THz}}(\omega)$; while for a PC antenna with a long carrier lifetime (for example, a semi-insulating GaAs PC antenna), $J(\omega) \propto E_{\text{THz}}(\omega)/\omega$. For ultrabroadband THz detection using a PC antenna with a finite carrier lifetime, the sensitivity at higher frequencies is thus expected to decrease (we also note that the structure of the PC receiver antenna may affect its spectral response, and that Kono *et al.*⁶ used a dipole-type antenna, different from the bowtie-type PC antenna used here). Nevertheless, PC detection still provides about eight times better signal-to-noise-ratio (defined as the ratio of the

peak amplitude of THz signal to the noise level) than EO-detection,⁸ up to frequencies in excess of 8 THz.

In conclusion, we have used LT-GaAs antennas for both generating and detecting ultrabroadband THz radiation. Our results show that such a PC-generation/PC-detection scheme leads to a smooth spectral distribution up to 8 THz and provides better signal-to-noise-ratio, compared with both EO-generation/PC-detection⁶ and PC-generation/EO-detection⁸ schemes. It thus makes an ideal system for THz time-domain spectroscopy in the frequency range 0.3–7.5 THz.

This work was supported by the Research Council UK (Basic Technology Programme), Toshiba Research Europe Ltd. (E.H.L.), and the Association of Commonwealth Universities (P.C.U.). I.S.G. and C.B. thank EPSRC for student-ship.

¹P. Y. Han and X.-C. Zhang, Appl. Phys. Lett. **73**, 3049 (1998).

²R. Huber, A. Brodschelm, F. Tauser, and A. Leitenstorfer, Appl. Phys. Lett. **76**, 3191 (2000)

³M. C. Beard, G. M. Turner, and C. A. Schmuttenmaer, J. Phys. Chem. B **106**, 7146 (2002).

⁴M. Tani, S. Matsuura, K. Sakai, and S. I. Nakashima, Appl. Opt. **36**, 7853 (1997).

⁵G. Zhao, R. N. Schouten, N. van der Valk, W. Th. Wenckebach, and P. C.M. Planken, Rev. Sci. Instrum. **73**, 1715 (2002).

⁶S. Kono, M. Tani, and K. Sakai, Appl. Phys. Lett. **79**, 898 (2001); **77**, 4040 (2000).

⁷T. A. Liu, M. Tani, M. Nakajima, M. Hangyo, and C. L. Pan, Appl. Phys. Lett. **83**, 1322 (2003).

⁸Y. C. Shen, P. C. Upadhyaya, E. H. Linfield, H. E. Beere, and A. G. Davies, Appl. Phys. Lett. **83**, 3117 (2003).

⁹I. S. Gregory, C. Baker, W. R. Tribe, M. J. Evans, H. E. Beere, E. H. Linfield, A. G. Davies, and M. Missous, Appl. Phys. Lett. **83**, 4199 (2003).

¹⁰P. C. Upadhyaya, Y. C. Shen, A. G. Davies, and E. H. Linfield, Vib. Spectrosc. **35**, 139 (2004).

¹¹M. Dauchez, P. Lagant, P. Derreumaux, G. Vergoten, M. Sekkal, and B. Sombret, Spectrochim. Acta **50A**, 105 (1994).